

Spatiotemporal selectivity of response to Notch1 signals in mammalian forebrain precursors

Christopher B. Chambers¹, Ying Peng¹, Hoang Nguyen¹, Nicholas Gaiano², Gord Fishell² and Jeffrey S. Nye^{1,*}

¹Departments of Molecular Pharmacology & Biological Chemistry and Pediatrics, Northwestern University Medical School, Chicago, IL 60611, USA

²Skirball Institute of Biomolecular Medicine, New York University, New York, NY 10021, USA

*Author for correspondence (e-mail: j-nye@northwestern.edu)

Accepted 8 December 2000; published on WWW 7 February 2001

SUMMARY

The olfactory bulb, neocortex and archicortex arise from a common pool of progenitors in the dorsal telencephalon. We studied the consequences of supplying excess Notch1 signal *in vivo* on the cellular and regional destinies of telencephalic precursors using bicistronic replication defective retroviruses. After ventricular injections mid-neurogenesis (E14.5), activated Notch1 retrovirus markedly inhibited the generation of neurons from telencephalic precursors, delayed the emergence of cells from the subventricular zone (SVZ), and produced an augmentation of glial progeny in the neo- and archicortex. However, activated Notch1 had a distinct effect on the progenitors of the olfactory bulb, markedly reducing the numbers of cells of any type that migrated there. To elucidate the mechanism of the cell fate changes elicited by Notch1 signals in the cortical regions, short- and long-term cultures of E14.5 telencephalic progenitors were examined. These studies reveal that activated Notch1 elicits a cessation of proliferation that coincides with an inhibition of the

generation of neurons. Later, during gliogenesis, activated Notch1 triggers a rapid cellular proliferation with a significant increase in the generation of cells expressing GFAP. To examine the generation of cells destined for the olfactory bulb, we used stereotaxic injections into the early postnatal anterior subventricular zone (SVZa). We observed that precursors of the olfactory bulb responded to Notch signals by remaining quiescent and failing to give rise to differentiated progeny of any type, unlike cortical precursor cells, which generated glia instead of neurons. These data show that forebrain precursors vary in their response to Notch signals according to spatial and temporal cues, and that Notch signals influence the composition of forebrain regions by modulating the rate of proliferation of neural precursor cells.

Key words: Neurogenesis, Gliogenesis, Telencephalon, Neural Progenitor, Subventricular Zone, Stem Cell, Neurosphere, Mouse

INTRODUCTION

The telencephalon gives rise to the cerebral neocortex, the archicortex, the olfactory bulbs (OBs) and subpallial structures. A common pool of adjacent cells segregates into distinguishable zones that generate these structures. The segregated precursors then give rise to neurons of various types and glia in a developmental sequence that is distinct for each structure and has been termed the spatiotemporal or neurogenetic gradient of differentiation (for a review see Jacobson, 1991). The capacity for multipotential fate is progressively restricted in normal development (Brock et al., 1998; McConnell, 1988) but is not entirely lost, as postnatal hippocampal cells retain the capacity to give rise to OB cells (Suhonen et al., 1996) and several neural cell lines can differentiate into various mature cortical cell types (Renfranz et al., 1991; Shihabuddin et al., 1995; Snyder et al., 1992). Following the generation of neurons, glia emerge. Recent work has indicated that soluble factors such as fibroblast growth factor (FGF), platelet-derived growth factor (PDGF) and

ciliary neurotrophic factor (CNTF) can regulate the decisions regarding which cell type to generate (Ghosh and Greenberg, 1995; Johe et al., 1996; Qian et al., 1997) from multipotent precursors. However, the identity of signals that control the potential of neural precursors in different regions of the forebrain and throughout developmental time is still poorly understood.

The Notch/lin12/glp1 (Notch) family participates in many diverse cell fate decisions in development predominantly as a signal that suppresses differentiation (Artavanis-Tsakonas et al., 1995). In development of the nervous system, the generation of neural precursors is restricted by Notch signaling (Coffman et al., 1993; Lewis, 1996; Nye et al., 1994). Notch signals are elicited in a cell when its Notch protein contacts the ligand for Notch of an adjacent cell. Ligands for Notch comprise the DSL family, for Delta, Serrate and Lag2 (for a review see Nye and Kopan, 1995). Studies in invertebrates have shown that the interaction of Notch and its ligands leads to the generation of two distinct cell types from identical precursors (Simpson and Carteret,

1990). *Notch1*, *Notch3* and *Delta1* (a Notch ligand) are expressed in the embryonic telencephalon during the period when regions segregate and commitment to cell types occurs (Lindsell et al., 1996). However, the role of these genes in forebrain development is still unclear.

In this study, we have asked how Notch signals affect the regional destination and cellular fate of telencephalic precursors, using bicistronic retroviral vectors. When injected embryonically, we found that activated Notch1 retroviruses inhibited the generation of neurons in all regions, and led to an increased generation of glia in the cortical regions. We also observed that activated Notch1 abolished the generation of OB cells, while it enhanced the generation of subventricular zone (SVZ) cells. Cultured neural progenitors infected with activated Notch1 entered an early quiescent phase followed by a proliferative phase, coinciding with a suppression of neurogenesis and an increase in the number of cells that expressed glial fibrillary acidic protein (GFAP). Postnatal injections into the anterior portion of the SVZ revealed that activated Notch1 transformed OB precursors into a quiescent, nonmigratory cell type that was reminiscent of stem cells. This study provides evidence that Notch signals regulate telencephalic progenitor fate during mammalian CNS development through its regulation of the proliferation of neural precursors.

MATERIALS AND METHODS

Retroviral vector construction

A replication-incompetent pLIA viral vector encoding an IRES sequence and human placental alkaline phosphatase was used as control virus (termed here IAP for IRES-alkaline-phosphatase) and a version expressing Notch1IC (Fig. 1, amino acids 1753 to 2531; Nye et al., 1994) was constructed (Notch1IC-IAP) as described previously (Bao and Cepko, 1997). A Myc epitope tag was present at the N terminus of the Notch1 cytoplasmic domain. A vector containing IRES-tau-lacZ (ITL) reporter was constructed by substituting the ITL sequence (Mombaerts et al., 1996) for the hPLAP gene in pLIA. A version (Notch1IC-ITL) was constructed with a Myc epitope-tagged Notch1IC truncated at the *Xho1* site (amino acids 1753-2185), and terminated by an oligonucleotide containing a stop codon (5'CGAGCTAGCTGATTAAT3').

Cell lines, virus preparation and titration

VSV-G pseudotyped retrovirus was prepared as described (Gaiano et al., 1999) using transient transfection and centrifugation. Viral concentrates were diluted to an equal concentration (1×10^7) and frozen in aliquots. The titers for the IAP and Notch1IC-IAP viruses were $1.2 \pm 0.05 \times 10^7/\text{ml}$ and $0.72 \pm 0.008 \times 10^7/\text{ml}$ ($n=10$) after this procedure. Infected fibroblasts were double stained as described below using anti-Myc (9E10) and either anti- β -galactosidase (5Prime \rightarrow 3Prime) or anti-alkaline phosphatase (Dako). In brain sections, the Myc epitope was detected using biotinylated 9E10 antibody to

reduce background (Nye et al., 1994). The biotinylated antibody was detected with avidin-biotin-peroxidase (Vector) and diaminobenzidine substrate.

Infection of embryos and harvest of brains

Timed-pregnant CD1 mice were obtained from Charles River and maintained on a 12 hour light/dark cycle with free access to food and water. All surgical procedures were performed in accordance with an approved institutional protocol. Mice were anesthetized with sodium pentobarbital (50 mg/kg, intraperitoneally) and MgSO_4 (1mg/10g). Sustained anesthesia during injections was achieved with metofane (Mallinckrodt Veterinary). The telencephalic vesicles of fetal mice were visualized by transillumination and were injected through the uterus with 1 μl of the viral supernatant containing 80 $\mu\text{g}/\text{ml}$ polybrene and 250 $\mu\text{g}/\text{ml}$ Fast Green dye as described (Cepko et al., 1995) under direct visual guidance. Embryos at E19.5 or mice at P9 and P21 were perfused transcardially with 10 ml of 4% paraformaldehyde in 0.1 M PBS buffer (pH 7.2) containing 2 mM MgCl_2 . Brains were removed, postfixed for 8-15 hours at 4°C, and cryoprotected in 30% sucrose. OCT-embedded brains were sectioned coronally on a Reichert Jung CM 3050 cryostat (Leica) and collected on slides in sets of serial sections at 40, 10, 10, 10, or 40, 40, 10, 10, 10, 10 μm , for the E19.5 brains and the brains at P9 and P21. Histochemical staining using either X-gal or X-phos reagents (Cepko et al., 1995) was performed on sections using standard techniques.

One set of 40 μm sections from the entire rostro-caudal distribution was scored for positively stained cells. This constitutes an unbiased sample of either 4/7 (E19.5) or 1/3 (P9 or P21) of the volume of a

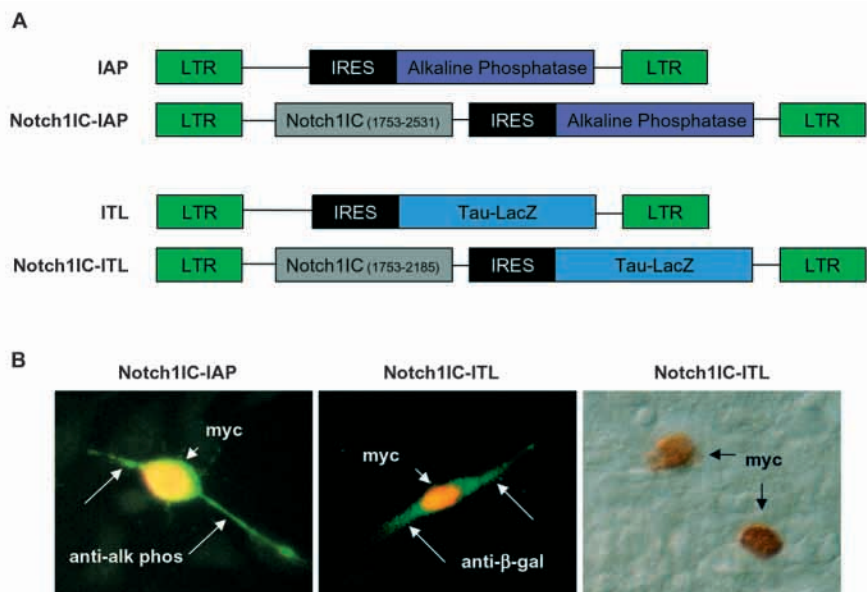


Fig. 1. Notch1IC retroviral vectors. (A) The structure of IAP, the control vector, is shown. An N-terminal Myc epitope-tagged Notch1IC (Nye et al., 1994) encoding residues 1753-2531 was inserted to create Notch1IC-IAP. The ITL virus was created by substituting IRES-bovine tau-lacZ into IAP in place of the PLAP gene. Notch1IC-ITL virus was truncated at a *Xho1* site and encodes Notch1 residues 1753-2185. (B) Double-label immunofluorescence of infected fibroblasts shows Myc antigen in the nucleus and alkaline phosphatase or β -galactosidase in the cytoplasm. Cells were infected with Notch1IC-IAP and stained with anti-alkaline phosphatase antibody (left) or Notch1IC-ITL and stained with anti- β -galactosidase (center), which were visualized with anti-rabbit FITC. Both cells were then stained with anti-Myc (9E10) mAb and visualized with anti-mouse Texas Red. Anti-Myc staining of a P9 hippocampal section from a brain infected at E14.5 with Notch1IC-ITL (right). Nuclear staining is detected, demonstrating expression of the Notch1IC protein. Biotinylated 9E10 antibody was visualized with avidin-biotin-peroxidase.

Table 1. Analysis of morphological identification of cells versus S100 β expression

	Morphological identification			Total
	Glial	Neuronal	Unidentified	
S100 β expression				
Positive (%)	172 (94.5)	2 (5.9)	0 (0)	174 (25.3)
Negative (%)	10 (5.5)	32 (94.1)	17 (100)	59 (25.3)
Total	182	34	17	233

Morphological identification of cells was tested for its ability to predict S100 β expression, a general marker for glia. Fetal brains were injected with ITL virus at E14.5, then harvested and sectioned at P21. Double label immunofluorescence staining with anti- β -galactosidase with anti-rabbit Texas Red and anti-S100 β with anti-mouse FITC was performed. Cells that showed a visible cell body in a single 10 μ m section were scored for morphological type while viewing Texas Red fluorescence, and were subsequently scored for the presence of S100 β using fluorescein. Sensitivity for detection of S100 β : 98.9% (S100 β -positive morphological glia/total S100 β positive cells). Specificity: 83.1% (S100 β -negative neurons or unidentified cells/total S100 β -negative cells). Predictive value of positive test: 94.5% (S100 β -positive glia/total morphological glia). Predictive value of negative test: 96.1% (S100 β -negative neurons or unidentified cells/total non-glia).

brain. Cells were assigned to one of seven regions: neocortical plate, white matter of the cerebrum, marginal zone of the cerebrum, OB, striatum, subventricular zone and archicortex. Each cell was categorized by morphology as neuronal, glial or 'unidentified', based upon their appearances after double staining (Table 1). Neurons were identified by characteristic axonal or dendritic processes and glia by either an astrocytic or oligodendrocytic appearance when visible, or as a glial cell of undetermined type.

Statistical analysis of labeled cells

The mean proportions for a scored category (region or cell type) were calculated by the number of scored cells divided by the total labeled cell counts for all three brains ($i=1$ to 3), i.e. mean proportion $p_{\text{virus}}=(\sum x_i)/(\sum n_i)$. The standard error (SE) was calculated by the weighted binomial formula $SE=[\sum n_i p_i (1-p_i)]^{1/2}/\sum n_i$ where x_i =the count of a region or of a cell type in a region in brain $_i$, $p_i=x_i/n_i$, (the proportion counted in brain $_i$) and n_i =the number of cells in brain $_i$. A Z statistic was calculated from the formula $[p_{\text{virus}1}-p_{\text{virus}2}]/[(SE_{\text{virus}1}^2+SE_{\text{virus}2}^2)^{1/2}]$. This method weights the data for the numbers of cells counted and was used to evaluate the null hypothesis that labeled cell counts from virus $_1$ and virus $_2$ were derived from the same normally distributed population, using a two-tailed test.

Double-label fluorescence immunocytochemistry

Cryostat sections (10 μ m) from ITL and Notch1IC-ITL brains were double labeled with rabbit anti- β -galactosidase (5Prime \rightarrow 3Prime; 1:500) and either mouse anti-S100- β (Sigma), mouse anti-CNPase (Sigma) or mouse anti-GFAP (ICN). Antigens were visualized with goat anti-mouse-FITC and goat anti-rabbit Texas Red (Jackson ImmunoResearch). Control or Notch1IC-infected brains were double labeled with rabbit α -alkaline phosphatase (Accurate Chemical and Scientific Corporation, 1:400) and NeuN (Developmental Studies Hybridoma Bank, 1:5) to detect neurons or RIP (Developmental Studies Hybridoma Bank, 1:20) to detect oligodendrocytes. Antigens were visualized with goat α -rabbit FITC and goat α -mouse Texas Red (both from Jackson ImmunoResearch), and mounted with Vectashield (Vector). Digital images were captured with an Orca camera (Hamamatsu) and assembled with OpenLab software (Improvision, Cambridge, MA).

Cryostat sections (20 μ m) from the postnatal injected animals (see below) were double labeled with sheep α -alkaline phosphatase (ARP; 1:250) and rabbit α -active caspase 3 (PharMingen, 1:250), to

determine infected SVZa-derived cells that were undergoing apoptosis. Antigens were detected with donkey α -sheep FITC and donkey α -rabbit Texas Red (both from Jackson ImmunoResearch); images were analyzed by laser-scanning confocal microscopy (Zeiss).

Cultures of E14.5 telencephalic precursors

The forebrains of E14.5 mouse embryos were dissected free of meninges and dissociated by trituration through a P1000 pipet tip. In the first set of experiments, neural progenitors (2.5×10^4 /well) were plated directly onto poly-L-ornithine (15 μ g/ml)/fibronectin (1 μ g/ml)-coated four-well chamber slides in serum-free media with supplements (DMEM/Ham's F12, 15 mM HEPES, N2 supplements) and 10 ng/ml basic (b) FGF (Gibco-BRL, Gaithersburg, MD). Progenitors were infected with retrovirus at a multiplicity of infection (MOI) of one at the time of plating and allowed to proliferate for 2 days. Media were changed and replaced without bFGF to accelerate differentiation, and 10 μ M BrdU was added. Cells were grown for 2 additional days before processing for indirect immunofluorescence.

In the second set of experiments, neural progenitors were grown as aggregates as described (Zhu et al., 1999). Briefly, the forebrains from E14.5 mouse embryos were dissected and dissociated as described above. Progenitors (4×10^5 /dish) were plated onto uncoated 6 cm tissue culture dishes in serum-free media plus 10 ng/ml bFGF and 2 ng/ml heparin and cultured for 6 days to generate aggregates. After 6 days in culture, aggregates were dissociated in 0.05% trypsin for 5 minutes, and washed and plated as single cells (2.5×10^4 /well) onto poly-D-lysine (20 μ g/ml)-coated 4 well chamber slides in serum-free media with 10 ng/ml bFGF. Progenitors were allowed to attach for 1 day, then infected with retrovirus (MOI=1) and grown for an additional 2 days in bFGF. After 2 days, bFGF was removed and the progenitors were cultured for 6 days. BrdU (10 μ M) was added 8 hours prior to processing the cells for indirect immunofluorescence.

Indirect immunofluorescence of cultured neural progenitors

Neural progenitors were fixed for 30 minutes in 4% paraformaldehyde, washed in PBS and blocked for 1 hour in 10% normal goat serum. Cells were then incubated with primary antibodies overnight at 4°C. The following primary antibodies were used: GFAP (rabbit polyclonal, 1:200, DAKO), β -tubulin (TuJ1, mouse monoclonal, 1:500, gift of L. Binder), human placental alkaline phosphatase (mouse monoclonal, 1:4000, Sigma), active caspase 3 (rabbit polyclonal, 1:100, New England Biolabs) and G3G4 (anti-BrdU, mouse monoclonal, 1:10, Developmental Studies Hybridoma Bank, Iowa City, IA). For BrdU staining, cells were incubated for 30 minutes in DNase (Roche Biochemicals) at 37°C then washed with Tris-EDTA buffer followed by PBS prior to incubation with the primary antibody. Cells were incubated with TR- and FITC-conjugated secondary antibodies (1:200) for 1 hour at room temperature with rocking. Isotype-specific secondary antibodies were used when appropriate (Southern Biotechnology Associates, Birmingham, AL). Images were obtained with a Zeiss Axioplan 2 microscope and an Orca (Hamamatsu) digital camera.

Postnatal injection of retroviral vectors into the anterior subventricular zone

Postnatal day 2 (P2) rat pups were anesthetized by ice water immersion and placed in a stereotaxic apparatus modified to stabilize neonatal rats. Retroviral preparation (1 μ l) was injected over a 5 minute period into the anterior subventricular zone (SVZa), defined by the following coordinates: 1.8 mm anterior, 1 mm lateral (both with respect to bregma) and at a depth of 2 mm (from the meningeal surface) (Luskin, 1993). Pups were perfused, brains were processed and sectioned as described above.

RESULTS

Pseudotyped defective retroviruses carrying activated Notch1

To accomplish both stable delivery of activated Notch1 and labeling of the cells carrying the vector, two types of bicistronic retroviral vectors (Lillien, 1995) were used (Fig. 1A). Notch1IC-IAP encodes an intracellular form of Notch1 (amino acids 1761-2531) followed by an encephalomyocarditis internal ribosomal entry site (IRES), and the cDNA for human placental alkaline phosphatase gene. Notch1IC-ITL encodes a Myc epitope-tagged truncated Notch1IC (amino acids 1761-2185; Nye et al., 1994) followed by an IRES and sequences encoding the tau- β -galactosidase fusion protein (ITL). For control viruses, the Notch1IC sequences were omitted (IAP and ITL viruses). VSV-pseudotyped retroviral stocks were prepared and concentrated (Gaiano et al., 1999). Virally infected 3T3 cells and infected brain cells demonstrated Notch1IC protein in the nucleus as detected by antibody to Myc, and either the tau- β -galactosidase or alkaline phosphatase proteins (Fig. 1B). Infected 3T3 cells were tested for the fidelity of co-expression of Notch1IC and β -galactosidase or alkaline phosphatase proteins, and 50/50 cells were positive for both (data not shown). This assures that cells assessed for expression of the histochemical marker also express Notch1IC polypeptide.

Activated Notch1 transiently delays emergence of cells from the SVZ

To determine the effect of Notch signals on precursor fates in the different structures of the forebrain, the telencephalic vesicles of mice in mid-neurogenesis (E14.5) were injected in utero with control or Notch1IC retroviral preparations. Following injections of each viral preparation, three mice were harvested at E19.5, P9 or P21, time points corresponding to the end of the major phase of neurogenesis (Boulder Committee, 1970), the end of postnatal astrocyte generation and the conclusion of oligodendrocyte generation, respectively (Levison et al., 1993; Levison and Goldman, 1993). The brains at these time points were processed histochemically; labeled cells were counted and scored for regional localization (Fig. 2, Table 2). For each time point and viral type we scored between 600 and 2100 labeled cells. The fractions of labeled cells in a region were compared with a binomial formula using a two tailed test of significance, as described in Materials and Methods.

In these experiments, we found a markedly altered pattern of labeled cells in the regions of the forebrain as a consequence of activated Notch1 (Notch1IC-IAP) retrovirus injected at E14.5 (Figs 2-4). A very similar regional profile was observed with Notch1IC-ITL virus (not shown). First, in areas where neurons represented a major fate of precursors (specifically, the OB, neocortical plate and striatum), a smaller fraction of labeled cells was seen at E19.5 and P9 after Notch1IC virus (Fig. 2A). This diminution in cells was only transient in the neocortical plate and archicortex, as brains harvested at P21 showed an equal or greater fraction of cells in the Notch1IC-infected brains compared with the control brains (Fig. 2C).

The second difference encountered after Notch1IC

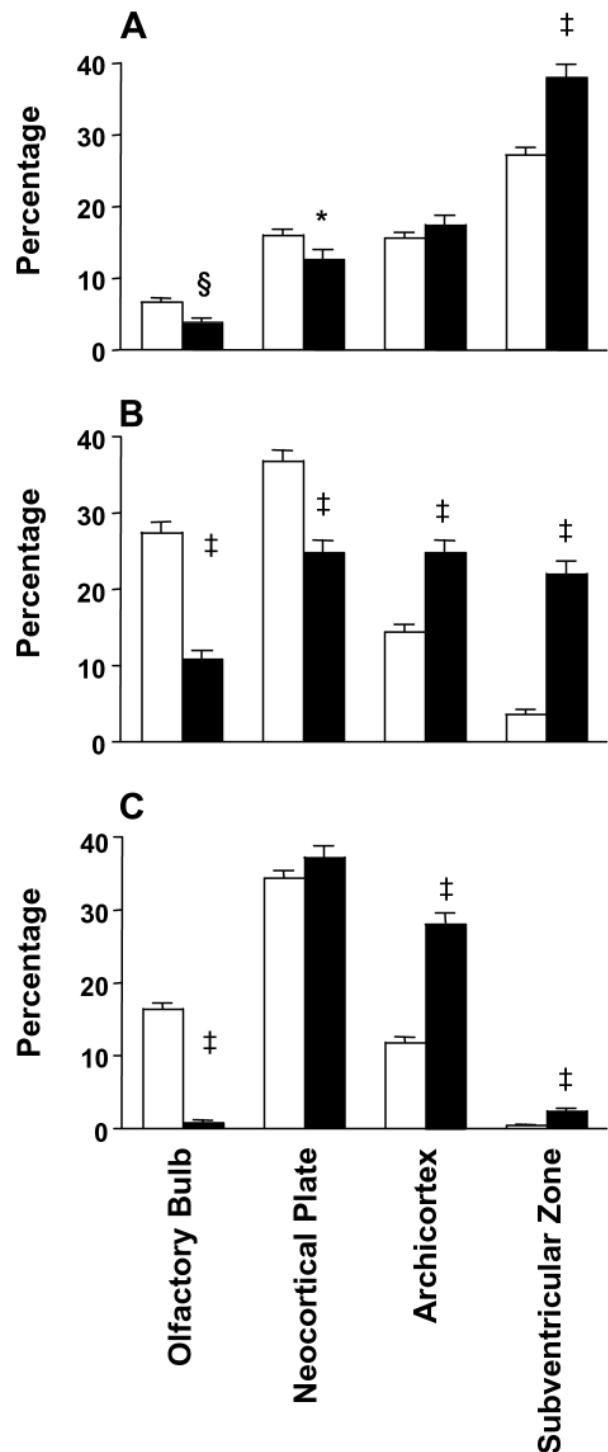


Fig. 2. Effect of activated Notch1 on the regional distribution of forebrain cells. (A-C) Fetal mouse telencephalic vesicles were injected with control (white bars, IAP) or Notch1IC (black bars, Notch1IC-IAP) retroviral preparations at E14.5 and harvested at E19.5 (A), P9 (B) or P21 (C). The brains were processed by X-phos histochemistry (see Materials and Methods) and labeled cells were scored for their regional distribution. Results are depicted as the proportion of pooled labeled cells in a region compared with total cells for three brains. Standard errors were determined using a binomial formula for three independent samples. The proportions of Notch1IC to control virus were compared using a two-tailed test by calculating a Z statistic. *, $P < 0.05$; §, $P < 0.01$; ‡, $P < 0.001$.

retrovirus infection was an enhancement in the fraction of labeled cells resident in the SVZ at all three time points (Fig. 2A-C). Following injection of retrovirus at E14.5, the SVZ was initially (at E19.5) the most heavily labeled region when either control or Notch1 virus was used (Fig. 2A). However, from P9 to P21, labeled SVZ cells declined as a percentage of total infected cells for the control virus (Fig. 2B,C). In contrast, Notch1IC-infected brains showed a decline, but it was slower than in control infected brains. A serial reconstruction of brains infected at E14.5 (Fig. 3) revealed that Notch1IC-injected brains showed a greater proportion of labeled cells in the SVZ at E19.5 and P9 compared with control injected brains. These data suggest that Notch1 activation produced a transient retention of cells in the SVZ and a corresponding delay in the appearance of cortical cells.

A similar delay in differentiation was seen in the archicortex. A reconstruction of the Ammon's horn from brains infected at E14.5 and harvested at P9 showed a dramatic increase in the number of cells located in the dentate gyrus ventricular region (Fig. 4A,B), which may represent the progenitor zone of the archicortex. A shift in laminar destiny was also apparent with few cells seen in the mature layers of the hippocampus and dentate gyrus compared with control virus (Fig. 4C). The mature cells mainly resembled astrocytic clusters (Fig. 4D). Small densely clustered cells were also observed following Notch1IC viral infection, similar to those seen in the cortical subventricular zone (not shown), but similar cells were never observed with control virus infection (Fig. 4C,D). Thus, activated Notch1 in the archicortex resulted in an increased fraction of precursor-like cells residing in the generative region of Ammon's horn.

With both Notch1IC-IAP and Notch1IC-ITL preparations, the clusters of cells in the SVZ or archicortex at E19.5 and P9 were difficult to quantitate accurately and were probably underestimated. Double immunofluorescence staining of the Notch1IC-infected SVZ cells at P9 did not reveal antigens characteristic of mature cell types (neurofilament, GFAP or RIP), and these cells were also negative for immature neural markers (nestin and TuJ1) (data not shown). However, at P21, many periventricular

clusters were positive for GFAP (Gaiano et al., 2000). The location in the cortical and archicortical generative zones and their capacity to generate mature cell types is consistent with a precursor cell phenotype.

Activated Notch1 suppresses the generation of all olfactory bulb cells from embryonic precursors

A third consequence of activated Notch1 virus on the regional distribution of cells was a marked reduction in the number of cells in the OB (Figs 2A-C, 3). At P21, virtually no cells were observed in the OB after Notch1IC infection. Serial reconstructions (Fig. 3) of Notch1IC-injected brains showed a virtual absence of Notch1IC-IAP-infected cells in the OB and rostral migratory stream (RMS) compared with control brains. This reduction of cells differed dramatically from the

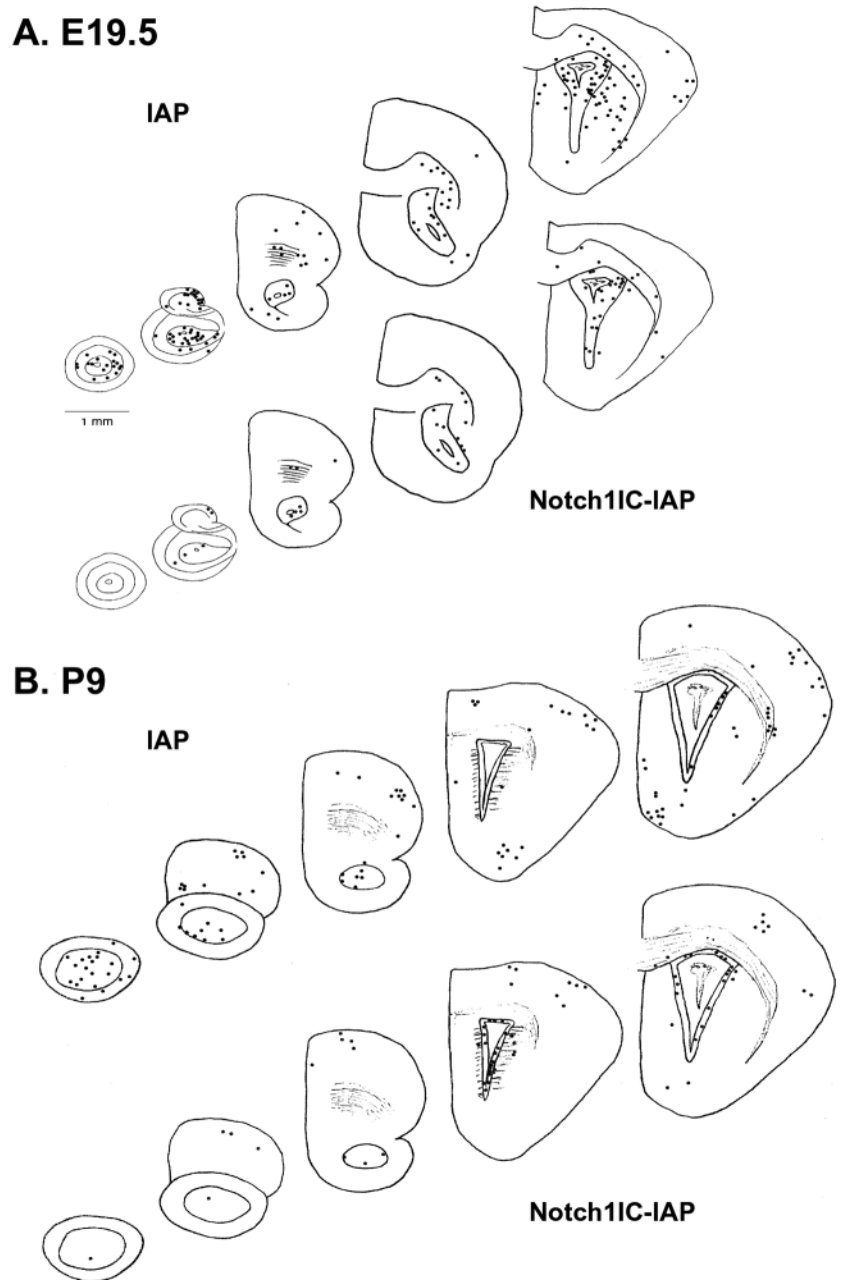


Fig. 3. Reconstruction of brains infected by Notch1IC and control retrovirus at E14.5. (A,B) Camera lucida reconstructions of the rostral half of two combined brains for each condition after infection at E14.5 with control (IAP) virus or Notch1IC-IAP virus, and harvest at E19.5 (A) or P9 (B). Sections spanning 210–480 μ m were condensed into each drawing. Numerous labeled cells are observed in the SVZ, RMS and OB in control infected brains (IAP). Labeled cells in Notch1IC-infected brains (Notch1IC-IAP) remain in the SVZ, and very few are observed in the RMS or OB.

Table 2. Labeled neurons and glia in regions of the telencephalon after retroviral infections at E14.5

	Embryonic day 19.5		Postnatal day 9		Postnatal day 21	
	IAP	Notch1IC-IAP	IAP	Notch1IC-IAP	IAP	Notch1IC-IAP
All regions	2141	653	1124	750	1940	863
% Neurons	7.4±0.6	2.0±0.5‡	31.1±1.4	7.1±0.9‡	25.2±0.9	0.4±0.2‡
% Glia					70.6±1.0	93.6±0.8‡
% Unidentified					6.2±0.5	4.3±0.7§
Olfactory bulb	140	24	309	82	320	8
% Neurons	38.6±3.7	20.8±7.9§	55.3±2.8	17.1±4.1‡	53.1±2.7	50.0
% Glia					26.3±2.4	37.5
% Unidentified					20.6±2.2	12.5
Neocortical plate	340	82	415	187	668	322
% Neurons	21.2±2.2	6.1±2.6‡	32.5±2.3	15.5±2.6‡	22.2±1.6	0.6±0.4‡
% Glia					75.6±1.7	98.4±0.7‡
% Unidentified					2.2±0.6	0.9±0.5
Archicortex	334	113	162	186	231	243
% Neurons	9.3±1.6	2.7±1.5*	27.2±3.3	5.4±1.6‡	44.6±3.2	5.3±1.4‡
% Glia					45.9±3.3	91.4±1.8‡
% Unidentified					9.5±1.8	3.3±1.1*

Control and Notch1IC viruses were injected at E14.5 into mouse telencephalic vesicles in utero and three brains were harvested and analyzed at each age indicated. Following sectioning, slides representing 4/7 (E19.5) or 1/3 (P9 and P21) of the volume of the brain were processed for X-phos staining. The total labeled cell counts are shown for three brains. Labeled cells were identified and scored as neuronal, unidentified (E19.5 and P9) or glial (P21) using morphological criteria. The fraction presented represents the number of labeled cells of a type as a percentage of cells counted in the region ± s.e. Standard errors are omitted where cell counts were zero. Significantly different from control virus: §, $P < 0.05$; *, $P < 0.01$; ‡, $P < 0.001$.

other neuron-containing regions of the telencephalon because it involved a decline in total cells (Fig. 2), not only neurons (see Fig. 6). In the OB, control retrovirus generated labeled neurons of various types (for example, see Fig. 5b) and glia that expressed S100β or GFAP (not shown). GFAP-positive astrocytes represented 19.8% of the ITL virus-expressing cells ($n=166$ cells counted) in P21 OBs infected at E14.5, but very few cells of any type were observed following Notch1IC retrovirus ($n=3$). Additionally, in brains infected with Notch1IC virus prenatally, we did not observe an accumulation of cells in the RMS, suggesting that the lack of OB cells was not due to a defect in cell migration. These data show that activated

Notch1 provided prenatally to telencephalic precursors can block the generation of OB cells.

Activated Notch1 diminishes the generation of forebrain neurons and enhances the size of glial clusters

Notch signals are well known to restrict progenitors from

Fig. 4. Composite camera lucida of hippocampal region cells infected with Notch1IC or control virus. (A,B) Composite of camera lucida drawings of the hippocampal region from P9 brains injected with control (A) and Notch1IC (B) after X-phos staining. Cells scored morphologically as neurons are red, glia are black and 'unidentified' are green. A marked reduction in the number of neurons and an increase in unidentified cells located in the ependymal zone is observed after Notch1IC-IAP virus treatment. Only mature appearing glia were identified. (C, D) Examples of X-phos-labeled cells located in the hippocampal region at P9 after retroviral injection into the telencephalic ventricle at E14.5 with control IAP (C) or Notch1IC-IAP (D) virus. Neurons, thin arrows; glia, arrowheads; unidentified cells, thick arrows; DGG, dentate gyrus granule layer; DGM, dentate gyrus molecular layer; DGP, dentate gyrus polymorphic layer; SLM, stratum lacunosum moleculare; SO, stratum oriens; SP, stratum pyramidale; SR, stratum radiatum.

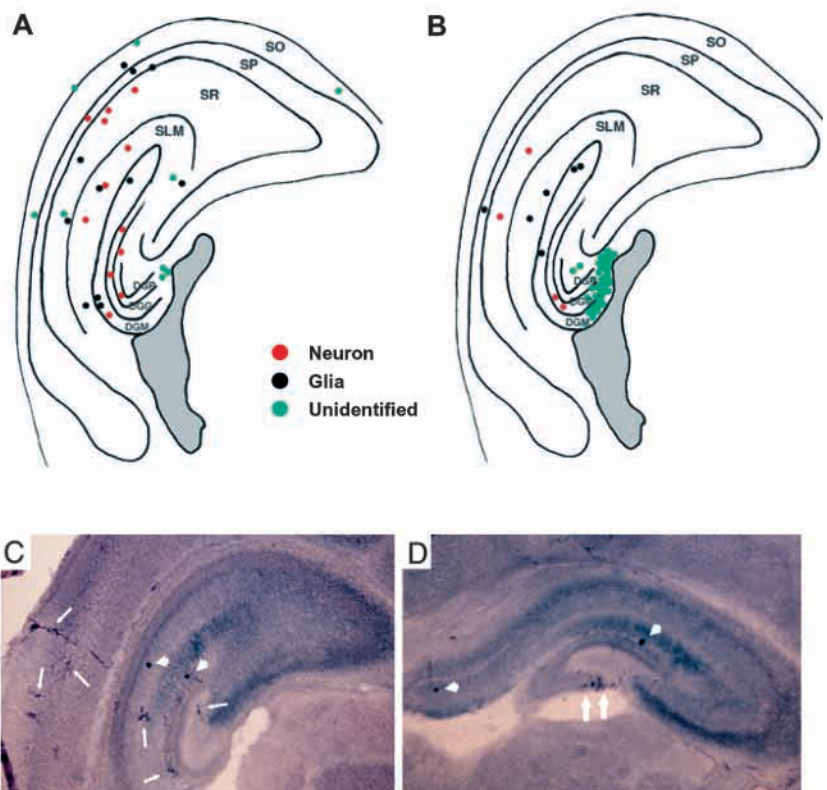
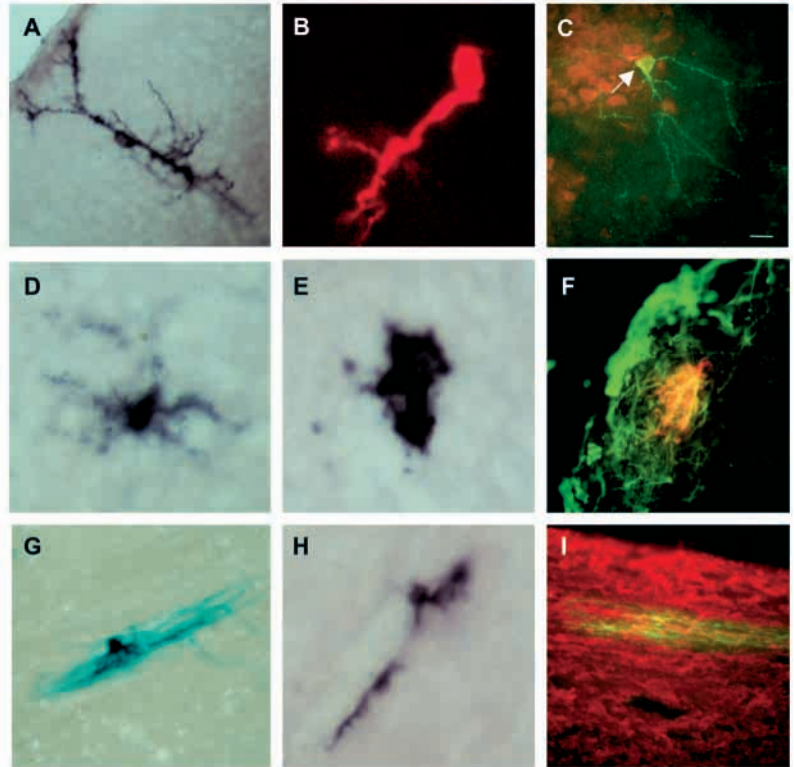


Fig. 5. Identification of cellular fates of activated Notch1-infected and control infected cells. (A-I) Examples of labeled cells at P21 after control (A-D,F,G,I) or Notch1IC (E,H) infections at E14.5. Labeled pyramidal neurons of the neocortex with IAP (A), interneurons of the OB (ITL, B) and hippocampal neurons (IAP, C) are seen with control virus, whereas virtually no neurons are seen with Notch1IC viruses (not shown). Labeled cortical astrocytes (D-F) were observed after infection with IAP (D,F) and Notch1IC virus (E, Notch1IC-IAP). Labeled oligodendrocytes (G,I) identified after control virus infection (G, ITL; I, IAP) and Notch1IC virus (H, Notch1IC-IAP) showed staining of myelin sheaths in the white matter. Brain sections were treated with either the X-gal or X-phos reagents to visualize the retrovirally infected cells. In B, anti- β -galactosidase staining was detected with anti-rabbit Texas Red. In C,I, anti-alkaline phosphatase is stained with FITC-conjugated antibody, and monoclonal antibodies to NeuN (C) and RIP (I) are stained with Texas Red-conjugated antibodies (see Materials and Methods). A double labeled neuron is depicted in C (arrow). In F, anti-alkaline phosphatase is stained with Texas Red-conjugated antibody, and GFAP is stained with FITC-conjugated antibody. Scale bar: 20 μ m.



choosing a primary neural fate in vertebrates and invertebrates (Artavanis-Tsakonas et al., 1995; Coffman et al., 1993; Lewis, 1996; Nye et al., 1994). To identify neurons and glia we used morphological criteria and confirmed the accuracy of our identification by double labeling for neuronal and glial markers. Neurons were identified morphologically by the presence of characteristic axonal or dendritic processes (Fig. 5A,B); this identification was confirmed in selected cases by the presence of NeuN staining (Fig. 5C). The control virus produced labeled neurons primarily in layers 3-5 of the neocortex and more superficial cortical interneurons, interneurons of the OB, and several types of neurons in the hippocampus and dentate gyrus (Fig. 5A-C). These neuronal types represent precursors making their final divisions at the time of viral injection based upon birthing studies (Caviness, 1982).

In accordance with prior experiments on primary neurons in vertebrates, Notch1IC retrovirus produced a marked reduction in the fraction of infected cells that became neurons in the OB, neocortical plate, archicortex (Fig. 6) and striatum (not shown), and at all three time points after E14.5 injection. These experiments demonstrate that Notch1IC largely abolishes the generation of neurons from all forebrain precursors, not just the primary neurons.

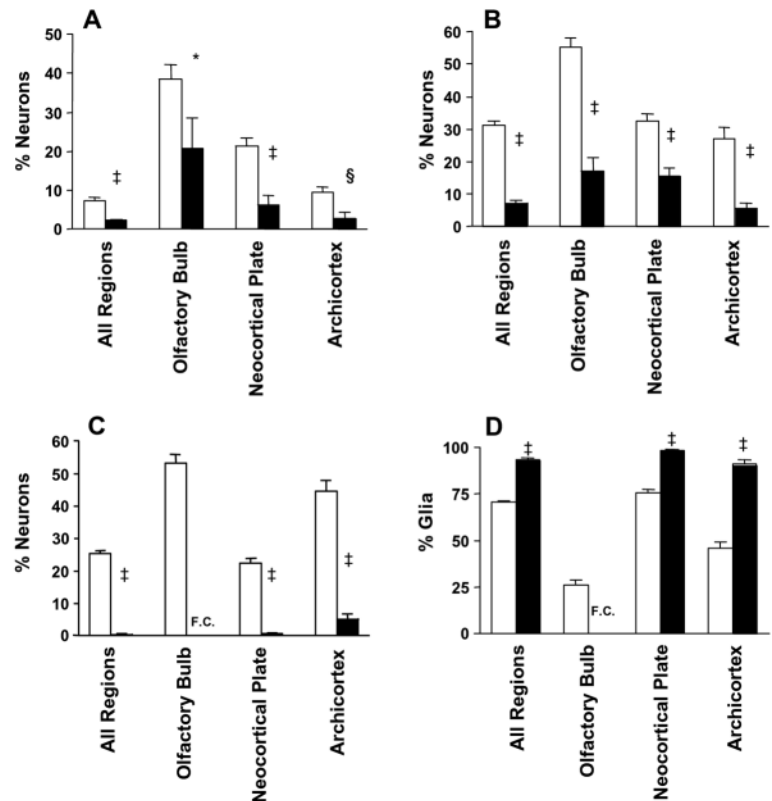
We previously observed a near total inhibition of neuronal generation in P19 embryonal carcinoma differentiation when individual cells that expressed nuclear Notch1IC were scored (Nye et al., 1994). In contrast, in this study we observed that a few neurons were repeatedly labeled with Notch1IC viruses (Fig. 6). It is possible that some fraction of the viral preparation did not transmit the Notch1IC gene product efficiently or that a window of susceptibility to Notch signals exists in neuronal precursors. Inhibitors of Notch signaling, such as Numb and numb-like, may be expressed at higher levels in these cells and

could possibly explain the emergence of some neurons in Notch1IC-injected animals (Wakamatsu et al., 1999).

To determine the effect of activated Notch1 on glial cells, glia were identified morphologically and the identifications were confirmed immunohistochemically in selected cases with GFAP for astrocytes, RIP and CNPase for oligodendrocytes, and S100 β as a general marker of CNS glia (Fig. 5D-I and not shown). An entire ITL-infected brain harvested at P21 was systematically screened to confirm the validity of our morphological identifications (Table 1). Because of the high sensitivity and specificity of the morphological identifications, and the technical ease of identifying many labeled cells, morphological identifications were used for a quantitative analysis of glia at P21 (Fig. 6d). We did not use the double labeling to compare Notch-infected brains because the yield of double-labeled cells was extremely low, owing to technical limitations of the virus and antibodies.

When the entire brain was scored, we observed a significant increase in the fraction of labeled glia following infection with Notch1IC virus when compared with control virus. This fractional increase in glia was most apparent for the neocortex and the archicortex, especially when brains were examined at P21. Most of the cortical plate glial cells infected with Notch1IC virus morphologically resembled large clusters of astrocytes (Figs 6E,F, 7) that expressed GFAP (Gaiano et al., 2000). We noted that the cluster size for astrocytes was larger after Notch1IC than control infection, based on the area occupied by each cluster (Notch1IC, $5.8 \pm 0.76 \mu\text{m}^2$, $n=37$; control, $2.7 \pm 0.31 \mu\text{m}^2$, $n=28$; $P < 0.05$, Student's *t*-test). Furthermore, the number of cell nuclei (as determined by Hoescht 33342 staining) within individual clusters of astrocytes was greater after Notch1IC infection than control infection (Notch1IC, 8.5 ± 1.23 , $n=15$; control, 3.4 ± 0.49 , $n=13$;

Fig. 6. Effect of activated Notch1 on neuronal and glial fates in the telencephalon. (A-D) Fetal mouse telencephalic vesicles were injected with control (white bars, IAP) or Notch1IC (black bars, Notch1IC-IAP) retroviral preparations at E14.5 and harvested at E19.5 (A), P9 (B), P21 (C) or P21 (D). The brains were processed by X-phos histochemistry and labeled cells were scored morphologically for cell types and regional distribution. Results are depicted as the proportion of labeled neurons (A-C) or glia (D) in a region compared with the total labeled cells in that region for three pooled brains. Standard errors were determined using a binomial formula for three independent samples. The proportions (Notch1IC versus control virus) were compared using a two-tailed test by calculating a Z statistic. *, $P < 0.05$; †, $P < 0.01$; ‡, $P < 0.001$; F.C., few cells (<1% of total).



$P < 0.01$ Student's *t*-test). This suggests that the relative increase in the glia after Notch1IC infection was due, at least in part, to the increased proliferation of astrocytes or astrocytic precursors. We did not analyze the fates of oligodendrocytes in detail.

Notch signals elicit cellular quiescence followed by glial proliferation in cultured telencephalon precursor cells

To elucidate the mechanism of the effects of Notch activation on neuronal and glial fates, we prepared cultures of E14.5 mouse telencephalic precursor cells and determined whether the rates of proliferation and cell death were affected by activated Notch1. We compared infections of the control retrovirus CLE (Gaiano et al., 1999), a replication defective retrovirus, and the CLEN retrovirus (Gaiano et al., 2000) which expresses a functional form of Notch1IC (amino acids 1753-2185) of mouse Notch1 followed by a C-terminal hexameric Myc epitope. These viruses also express alkaline phosphatase bicistronically from the IRES. We studied these viruses in two sets of culture conditions, short-term cultures that showed neurogenesis, and longer-term cultures that showed both neuronal and glial generation from individual neural progenitors.

In the first set of experiments, we examined cultures that were plated immediately upon dissociation, infected with retrovirus, and grown in bFGF for 2 days (Fig. 8A). Differentiation was accelerated by culturing the cells for an additional 2 days in the absence of bFGF and bromodeoxyuridine (BrdU) was added to label cells that proliferated in this period. Double labeling with an antibody to alkaline phosphatase (to identify infected cells) and anti-BrdU (to mark proliferative cells) revealed that the majority of infected cells in both cultures were proliferating following infection (Fig. 8B, arrows; Fig. 8C). However, in Notch1IC infected cultures, a significant fraction of AP-positive cells were BrdU negative (Fig. 8B, arrowhead; Fig. 8C), indicating that they were quiescent. In contrast, control infected cultures showed only a small fraction of alkaline phosphatase-positive cells that were BrdU negative, indicating that very few quiescent cells were present. No differences were observed in the rate of infection by retrovirus. The production of quiescent cells by Notch1 activation coincided with a decline in the number of alkaline phosphatase-positive neurons (see below). However, uninfected cells in the same culture did give rise to neurons (Fig. 8B, asterisks) indicating the specificity of the effect of

Notch1IC virus. The AP⁺/BrdU⁻ cells elicited by Notch1IC virus were primarily large flat cells that were negative for GFAP expression (Fig. 8B, inset and not shown). To establish whether these or other Notch1IC-infected cells were targeted for cell death, we examined the expression of activated caspase 3, an early marker of apoptosis. While 32-39% of the cells in short-term cultures contained activated caspase 3, less than 1% of control or Notch1IC-infected cells did so. No caspase 3-expressing cells were among the large flat cells induced by Notch1IC. These studies indicate that Notch signals inhibit neurogenesis in part by driving precursor cells into a quiescent, non-apoptotic cellular phenotype that fails to generate neurons.

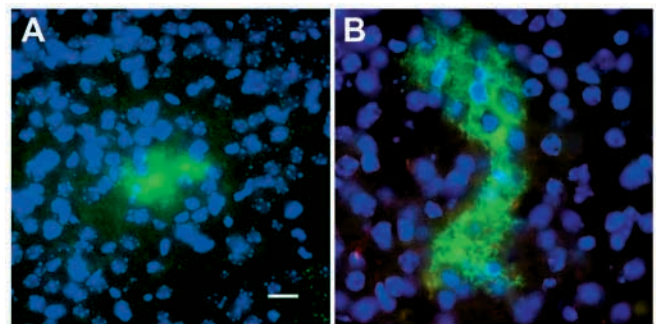


Fig. 7. Effect of activated Notch1 on glial clusters. (A,B) Indirect immunofluorescence of control (A) and Notch1IC- (B) infected cells at P9 labeled with α -alkaline phosphatase and FITC-conjugated α -rabbit secondary antibody; nuclei (blue) were detected by Hoechst 33342. Notch1IC retroviral infection produced glial clusters of increased size when compared with the control retrovirus at P9. Scale bar: 20 μ m.

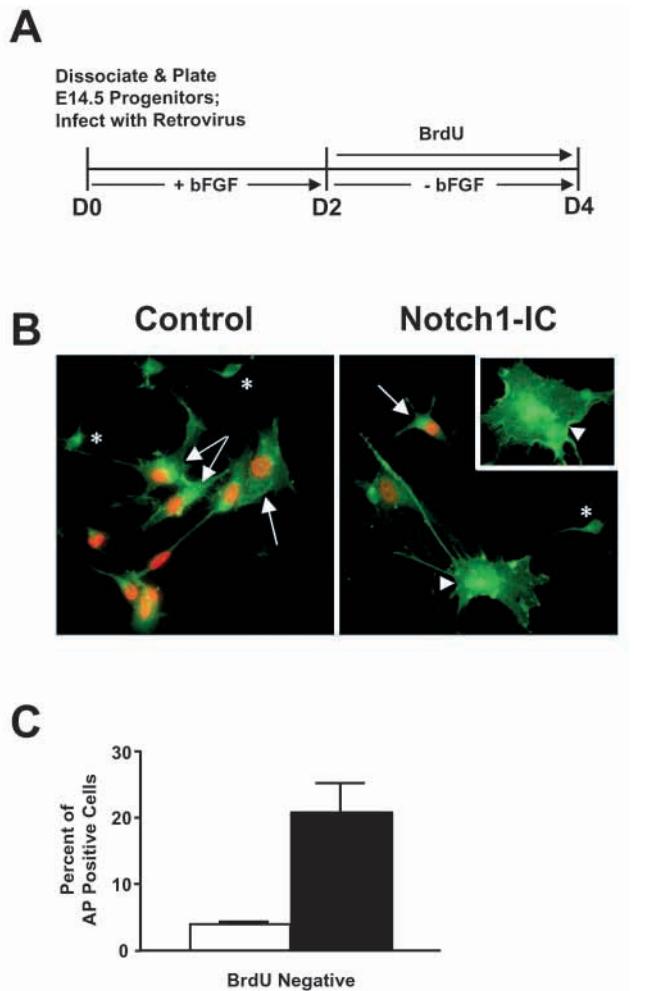


Fig. 8. Production of quiescent neural precursors by Notch1IC retrovirus in short-term cultures. (A) Timecourse of short term neural precursor cultures. See Materials and Methods for detailed conditions. (B) Double-labeled immunofluorescence for alkaline phosphatase and BrdU. The majority of progenitors infected with the control virus were positive for both alkaline phosphatase and BrdU (arrows), while a population of progenitors infected with the Notch1IC virus were alkaline phosphatase positive but BrdU negative (arrowheads). These cells were typically large and flat. Additionally, cells with a neuronal morphology were present in both cultures (asterisks). Inset depicts another typical alkaline phosphatase positive/BrdU negative cell. (C) Quantitation of the fraction of infected (alkaline phosphatase positive) cells that were not proliferative (BrdU negative). These data reveal that the Notch1IC virus produced a greater number of quiescent cells (BrdU negative) than did the control virus (two independent experiments; $P < 0.05$).

In a second set of experiments designed to observe the fates and the rate of proliferation from cultured neural precursors that generated neurons and glia, we prepared dissociated neural progenitors from E14.5 telencephalon and grew them in bFGF for 6 days (Fig. 9A). This culture condition generated aggregates, sometimes called neurospheres (Reynolds and Weiss, 1992), that were then dissociated into single cells. These cells were plated and infected with control or Notch1IC retroviruses (CLE or CLEN), and then induced to differentiate for an additional 6 days in the absence of bFGF. After 15 days

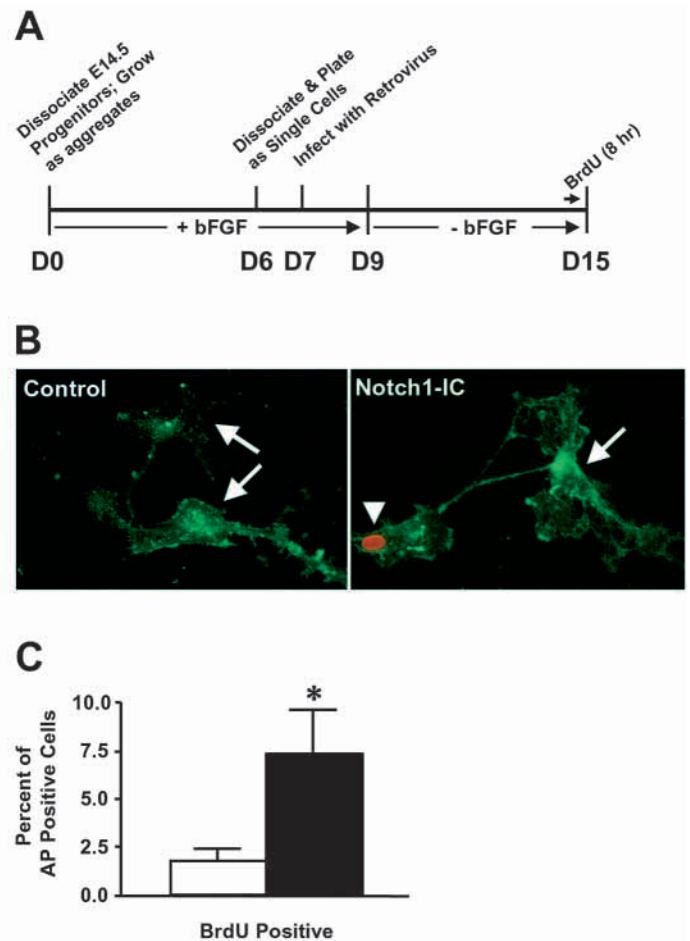


Fig. 9. Enhancement of proliferation by Notch1IC retrovirus on 16-day telencephalic cultures. (A) Time course of long-term cultures. See Materials and Methods for details. (B) Double-labeled immunofluorescence for alkaline phosphatase and BrdU. While the majority of control infected progenitors were BrdU negative (arrows), a subpopulation of Notch1IC infected progenitors were positive for both alkaline phosphatase and BrdU (arrowhead). (C) Quantitation of the fraction of infected (alkaline phosphatase positive) cells that were proliferative (BrdU). These experiments reveal that the Notch1IC virus produced a greater number of proliferative cells at a late developmental time point than did the control virus (two independent experiments; $P < 0.05$).

in culture, the cells were labeled with BrdU for 8 hours and then double stained with anti-BrdU and anti-alkaline phosphatase antibodies to assess the rates of proliferation. In contrast to the results with short-term cultures, we observed that the long-term cultures infected by the activated Notch1 virus contained a significantly greater fraction of BrdU-labeled cells than control infected cultures (Fig. 9B,C).

To examine the effect of Notch1IC on cell fates in the long-term cultures, wells were double labeled with an antibody against neuron-specific tubulin (TuJ1) (Fig. 10A), or an antibody against GFAP (Fig. 10B). The fraction of infected cells that expressed TuJ1 was significantly higher with the control retrovirus than with the activated Notch1 virus (Fig. 10C). However, the fraction of infected cells expressing GFAP was markedly higher for Notch1IC-infected cells than for those infected by control virus. Therefore, similar to the *in vivo*

retroviral injections, activated Notch1 virus diminished the numbers of neurons and increased the generation of astroglial cells from telencephalic precursors. Since long-term cultures showed an increased rate of proliferation following Notch1IC virus treatment, we propose that the greater numbers of glia found after Notch1 activation is a consequence of both the restriction of neuronal fates and the increased rate of glial proliferation.

Activated Notch1 blocks the maturation of OB precursors postnatally

Luskin (1993) and others have shown that the anterior segment of the postnatal SVZ (SVZa) is a specialized source of cells that migrate along the RMS, enter the OB and differentiate mainly into interneurons of the OB. Other studies indicate that the early postnatal SVZ is a source of cortical glia (Levison and Goldman, 1993; Paterson et al., 1973). Therefore, to delineate the effect of Notch signals on precursors of the OB, we injected the Notch1IC (Notch1IC-IAP, Fig. 1) and control retroviruses stereotactically into the SVZa of rats at P2, and examined the number of infected cells in the SVZa, RMS and OB at P4, P7 and P21 (Fig. 11). Compared with control,

retroviral Notch1IC injections produced a markedly lower number of labeled cells at P4 and P7 (Figs 11, 12). At P4, the total number of labeled cells produced by the Notch1IC virus was 27 times less than control (Notch1IC, 0.11×10^{-2} cells/virion/brain; control, 3.1×10^{-2} cells/virion/brain). A similar reduction in labeled cells was apparent at P7. To assure that the reduced rate of labeled cells was a selective effect of activated Notch1 on SVZa precursors and not an error in injection or a toxic effect of the viral preparation, we injected a mixture of β -galactosidase-expressing retrovirus (BAG) and Notch1IC-IAP or control IAP virus into the P2 SVZa. After Notch1IC-IAP/BAG virus co-infection, numerous β -galactosidase-positive cells, but few or no alkaline phosphatase-positive cells, were found in the SVZa and RMS in double-stained sections at P4. In contrast, IAP-virus/BAG virus co-mixtures gave equivalent populations of cells stained for either histochemical marker (data not shown). Additionally, the Notch1IC virus preparations used were the same ones that gave large numbers of SVZ clusters following E14.5 injections (above) and titers on 3T3 cells were checked before and after injection. We therefore conclude that the vast majority of SVZa precursors infected by the Notch1IC retrovirus selectively failed to proliferate or were eliminated immediately after Notch1IC expression.

A rapid rate of proliferation has been noted for cells of the postnatal SVZ and RMS. Accordingly, in control injected animals we observed a 25.9-fold increase in the number of labeled cells along the RMS and in the OB from P4 to P7, followed by a subsequent decline in labeled cells by P21 (Fig. 11). The decline in labeled cells between P7 and P21 may be attributable to cell death, as apoptosis appears to be a common fate of cells in the RMS and SVZa (Brunjes and Armstrong, 1996; Morshead and van der Kooy, 1992). In contrast to cells expressing the IAP virus, cells of the SVZa-expressing retroviral Notch1IC proliferated more slowly and remained confined to the SVZa. When the total number of

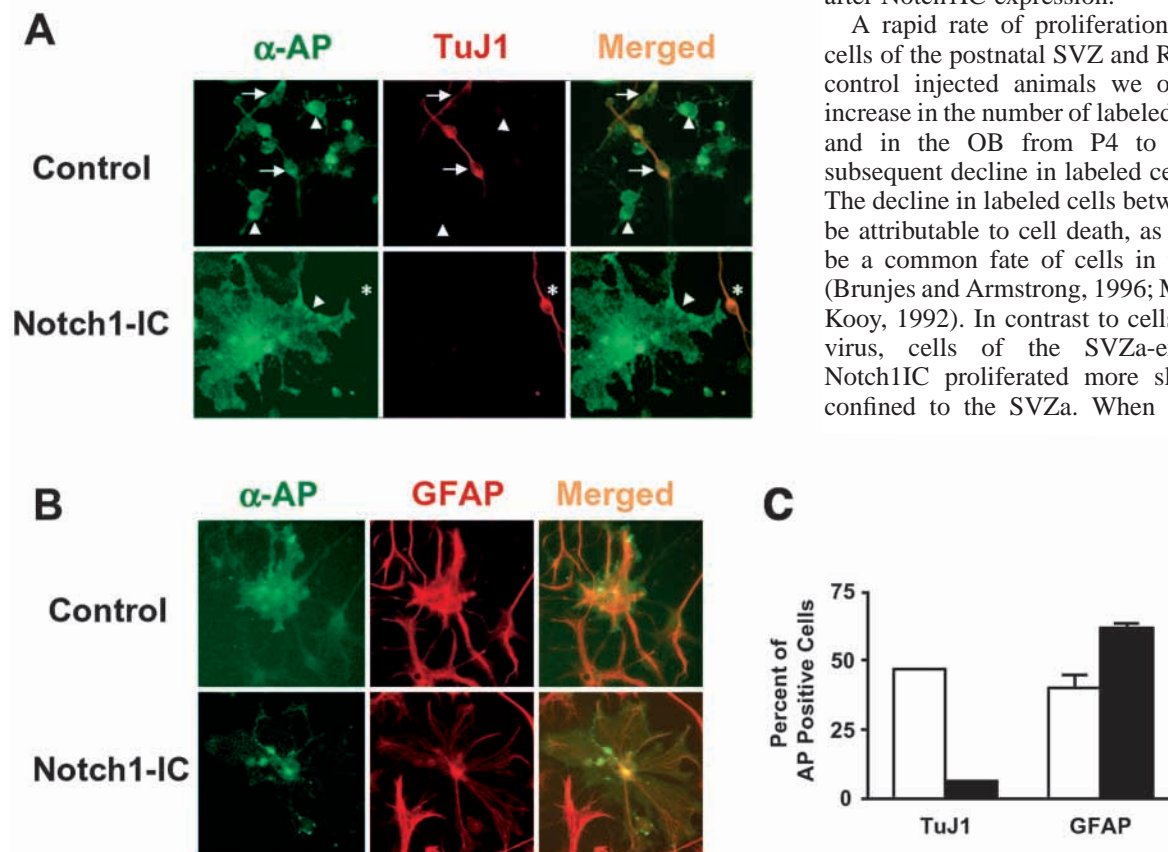


Fig. 10. Cell fates of long-term neural precursor cultures in response to activated Notch1 virus. Neural progenitors were cultured for 15 days, as described, and stained with antibodies specific for neurons (TuJ1) or astroglia (GFAP). (A) Double labeling for infected (alkaline phosphatase (AP) positive, green) neurons (TuJ1 positive, red). Control infected progenitors gave rise to TuJ1-positive neurons (arrows) and non-neuronal cells (arrowheads). Notch1IC-infected progenitors produced few TuJ1-positive cells (not shown), but AP-negative/TuJ1-positive cells (asterisk) were present in the Notch1IC-infected cultures. A non-neuronal AP-positive cell is shown (arrowhead). (B) Control and Notch1IC-infected progenitors produced many GFAP-positive cells. In double-stained cells, antibody to AP stains the plasmalemma, while GFAP stains intermediate filaments. (C) Quantitation of cell type double labeling. Notch1IC greatly decreased the number of TuJ1-positive cells and increased the number of GFAP-positive cells produced by E14.5 neural progenitors.

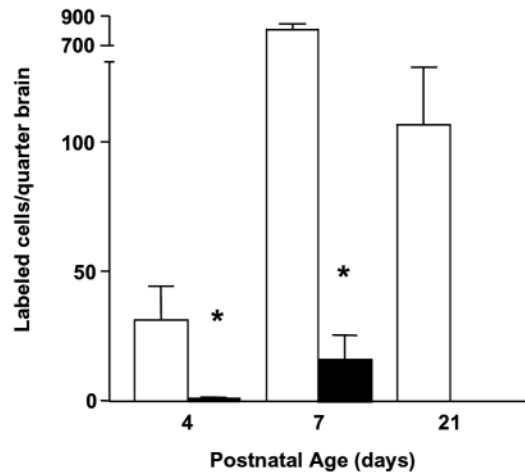


Fig. 11. Quantitation of cells after Notch1IC and control infections of anterior SVZ at postnatal day 2 in the rat. Control (white bars) and Notch1IC (black bars) retroviruses were stereotactically injected into the SVZa of P2 rats. Animals were sacrificed 2, 5 and 19 days after injection; brains ($n=3$ for each virus) were removed and processed for X-phos histochemistry. Infected cells were counted in the SVZa, RMS and OB, and compared with Student's *t*-test. Notch1IC produced fewer X-phos-positive cells than did control at all time points examined (*, $P<0.05$).

Notch1IC-expressing cells was compared between P4 and P7, a slower rate of increase was observed (16-fold) compared with control (26-fold). Additionally, 73 out of 75 cells ($n=3$ brains) expressing Notch1IC remained in the SVZa, compared with control infections, where >90% had migrated into the RMS or OB. No cortical glia were observed after Notch1IC virus,

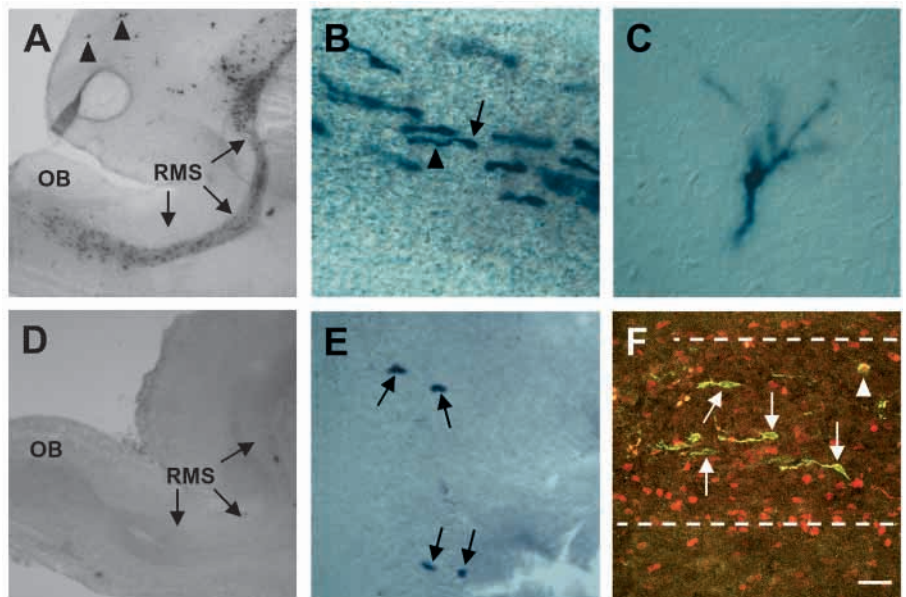
demonstrating that the effect on postnatal SVZ cells was not merely an effect on the ability to migrate. These data suggest that Notch1IC slowed the rate of proliferation and prevented SVZa precursors from generating differentiated progeny.

Phenotype of SVZa cells expressing an activated Notch1

The distribution of cells expressing alkaline phosphatase following control virus injection into the SVZa at P2 consisted mainly of cells located in the SVZa, followed by cells migrating along the RMS, and, finally, cells predominantly in the OB (Fig. 12A-C) as noted by previous investigators (Luskin, 1993). Control virus also produced cells migrating to the cerebral cortex that resembled glia (Fig. 12A, arrowhead). In contrast, the Notch1IC-expressing cells were small and round (as labeled by alkaline phosphatase), and did not elaborate a migratory profile (compare Fig. 12B with 12E). They did not express GFAP or neuron-specific tubulin (TuJ1) in double label experiments (not shown). Based upon their location in the SVZ and their morphology, Notch1IC-expressing cells resemble stem cells that have long cell cycle times and reside in the adult SVZ (Doetsch et al., 1999; Morshead et al., 1994; Morshead et al., 1998). Since these cells grew in number from P4 to P7 without generating differentiated progeny or migrating out of the SVZa, we conclude that they remained as slowly dividing precursor cells that failed to make asymmetrical divisions.

Typically, precursor cells in the SVZ make asymmetrical divisions to generate committed OB neuroblasts, and some fractions die by programmed cell death (Brunjes and Armstrong, 1996; Morshead and van der Kooy, 1992). We examined the postnatal brains after SVZa infection and found that 8.5% of control retrovirus-infected cells were undergoing

Fig. 12. Effect of retroviral Notch1IC on postnatal anterior SVZ cells entering the rostral migratory stream. Control (A-C,F) or Notch1IC-IAP (D,E) viruses of equivalent titer were stereotactically injected into the SVZa of P2 rats and brain sections were stained with X-phos reagents. Low-power view of a sagittal section from a control injected brain (A) at P7 reveals numerous labeled cells in the SVZa, RMS and OB. Low-power view of a sagittal section from a Notch1IC-injected brain (D) at P7 reveals very few labeled cells in the same regions. Cells within the RMS of a control injected animal (B) show a typical migratory morphology with a leading process (arrowhead) extended from the cell body (arrow) in the direction of migration (the OB is towards the left). These cells migrate to the OB, where they differentiate into granule cell layer (not shown) and periglomerular (C) interneurons (image taken from a P21 control injected animal). While the Notch1IC retrovirus produces much fewer labeled cells than does the control retrovirus, a few labeled cells are present in the SVZa of Notch1IC-injected animals (E, arrows). Note the lack of leading processes or other differentiated features. (F) A subpopulation of SVZa-derived cells undergo apoptosis in the RMS. An infected cell (arrowhead) stained with α -alkaline phosphatase (detected with α -sheep FITC) located in the RMS of a control retrovirus injected animal double-labeled with α -active caspase 3 antibody (detected with α -rabbit Texas Red). Note that the double-labeled cell lacks a migratory morphology, in contrast to the migratory character of those α -alkaline phosphatase positive cells that lack caspase 3 staining (arrows). Broken white lines indicate the lateral extent of the RMS. Scale bar: 20 μ m.



apoptosis at P7, as indicated by the co-expression of alkaline phosphatase and active caspase 3 proteins in these cells (15 double-labeled out of 192 α -alkaline phosphatase positive; Fig. 12F). Both cells with migratory profiles (33%) and those that were round and precursor-like (67%) showed activated caspase 3 expression. In contrast, we did not observe any activated caspase 3 immunoreactivity among the Notch1IC-expressing cells. Taken together, these results suggest a model in which Notch1IC converted OB precursors residing in the SVZa into a nonmigratory, slowly dividing, undifferentiated phenotype.

DISCUSSION

The present study demonstrates that the response of neural precursors *in vivo* to Notch signals depends upon the regional localization within the telencephalon and the time of exposure to the Notch signal. Following the expression of activated Notch1 in mid-gestation, proliferating cells of the neo- and archicortex transiently persist as SVZ precursor cell types, but then generate primarily glia in increased numbers. A mechanism for the delay in differentiation and apparent enhancement in glial numbers was revealed by *in vitro* experiments. Notch activation initially elicits a cessation of proliferation without differentiation during the phase of neuronal generation, but when glia are being generated, Notch activation accelerates their rate of proliferation. Although Notch signals appear to promote glial fates in several systems (Furukawa et al., 2000; Gaiano et al., 2000; Morrison et al., 2000), including the neo- and archicortex (this study), Notch signals direct precursors of the early postnatal OB to lose their capacity to generate mature cells and they remain nonmigratory and quiescent, reminiscent of stem cells. Thus, Notch signals suppress neurogenesis and either promote gliogenesis or promote the persistence of stem-like cells. These variations in response to Notch signals imply that the forebrain uses the Notch pathway in multiple ways, depending upon the competence of the cell receiving the signal.

Notch signals and neural fates in cortical regions

Cortical precursors generate multiple neuronal cell layers in a temporal sequence, followed by the generation of cortical glia. Cortical neurogenesis in the mammal has been termed secondary neurogenesis because it overlays the primary neuronal scaffold characteristic of lower vertebrates (Marin-Padilla, 1978). The present studies suggest that the telencephalon uses Notch signals to restrict its generation of neuronal populations, as previously observed in invertebrate and vertebrate primary neurogenesis (Chitnis et al., 1995; Coffman et al., 1993; Lewis, 1996). Unlike primary neurogenesis, however, the negative regulation afforded by Notch signals is probably needed in the layered cortical structures to assure a supply of precursors for later steps in their developmental pathway when additional neuronal types are generated (Dorsky et al., 1997; Lewis, 1996). Notch-Delta signaling regulates the formation of diverse cell types in the layered retina (Dorsky et al., 1997; Henrique et al., 1997). The analogy between the forebrain and the retina is particularly instructive because both structures have layers that emerge from common precursors in a spatiotemporal gradient. Moreover, the role of Notch in generating a diversity of cell

types was observed early on in *Drosophila* development (Cagan and Ready, 1989; Hartenstein and Posakony, 1990; Shellenbarger and Mohler, 1978).

A detailed view of the inhibitory effect of Notch signals on the telencephalon is provided by the present studies. We observed that Notch1IC delayed the maturation of SVZ cells underlying the neo- and archicortex at a time when the predominant cell type being generated was neuronal. The consequence of this delay in differentiation was persistence of precursor cell types in the SVZ that were phenotypically small and formed large clusters. We found that these precursor-like cells gradually diminished from P9 to P21 after embryonic injections. Concurrently, the number of glia emerging as a consequence of activated Notch1 increased with age, indicating that the Notch signals contributed to promoting a glial fate from precursor cells of the SVZ. Glial cluster size was also increased, suggesting a higher rate of proliferation of glia or glial precursors.

The *in vitro* experiments offer a mechanistic explanation for both the inhibition of neurogenesis and the increased proliferation of glia. Notch activation produced a virtual elimination of neurons and an increased generation of glia *in vitro*, as well. First, the short-term cultures afforded a glimpse into the consequences of Notch signals on cell fates early in the differentiation of telencephalic precursors. Notch activation elicited both inhibition of neurogenesis and a population of quiescent cells that were not apoptotic. We suggest, but have not proven, that the quiescent cells were indeed the same neural precursors that were prevented from neuronal generation by Notch signals. This conclusion is appealing because the fraction of the total infected cells that were shifted to a quiescent state corresponded closely to the fraction that typically become neurons (~10%) in these cultures. The observation that neural precursors in which Notch was activated are not destined for apoptosis implies that Notch signals do not trigger the death of neural precursors in order to restrict neurogenesis. Instead, it appears that Notch signals trigger a cessation of proliferation that corresponds to a restriction of neuronal generation.

Although it is appealing to apply the conclusions derived from the *in vitro* studies to the *in vivo* results, it is also possible that other mechanisms, such as a death of neurons might explain some of our results. For instance, the decline of neocortical neurons infected by Notch1IC virus from ~15% to ~1% in the interval from P9 to P21 could possibly be a consequence of the enhanced proliferation of other cells. However, another intriguing possibility is that neurons that make abnormal processes, as a result of excess Notch signals, do not survive (Franklin et al., 1999; Sestan et al., 1999). Thus, we cannot exclude the possibility that cell death plays a role in the *in vivo* cell number changes without a corresponding study of cell death *in vivo*.

The result of Notch signals in the telencephalon, *in vivo* and *in vitro*, was an apparent promotion of glial differentiation. This fits with recent studies showing that Notch signals promote the differentiation of radial glia, peripheral glia and retinal (Müller) glia (Furukawa et al., 2000; Gaiano et al., 2000; Morrison et al., 2000) in the vertebrate nervous system. A switch to a glial fate was previously observed in the *Drosophila* PNS (Hartenstein and Posakony, 1990; Jan and Jan, 1990). Since Notch signals operate by the activation of

transcriptional elements, the observation that multiple types of glia arise after Notch signaling implies that a factor that is essential for glial differentiation may be a direct or indirect target gene of Notch signal transduction.

However, the present studies reveal that the apparent promotion of glia arises in two steps in cells that are competent to generate glia. First, Notch induces a phase during which quiescent neural precursors may be respecified to glial precursors. Subsequently, glia or glial precursors show higher proliferative rates. We have not determined what factors control the quiescent versus the proliferative response to Notch signals, and note that radial glial clusters were either rapidly proliferating or quiescent following Notch activation (Gaiano et al., 2000). A recent study has suggested that Notch signals act instructively rather than permissively to promote glia (Morrison et al., 2000). This is supported by the observation that neural crest precursor cells acquire a rapid and heritable shift in their fate following a brief activation of their Notch receptors. However, a transient quiescent phase followed by enhanced proliferation of glia or glial precursors would probably resemble an acceleration of glial differentiation, even though it is more complex rather than a purely instructive signal. Although instructive, glia-inducing signals may play a role in the terminal fates of certain neural precursors, many examples exist in which multipotent neural precursors do not respond to Notch signals with gliogenesis (Cagan and Ready, 1989; Dorsky et al., 1997; Henrique et al., 1997). In line with these precedents, the present study demonstrates that postnatal SVZa cells respond to Notch signals with quiescence rather than gliogenesis. Thus, the diversity of response to Notch signals favors a permissive, rather than an instructive role in neural development in many cases.

The proposed role of the Notch pathway in cortical cell fates is consistent with the observation that Notch1, Notch 3 and Delta1 are expressed in the telencephalon in mid-neurogenesis in rodents (Lindsell et al., 1996; Zhong et al., 1997), and that Numb has a role in modulating Notch signals in chick cortical development (Wakamatsu et al., 1999). Understanding the exact cellular distribution of these components would aid considerably in discerning which cells were receiving Notch signals at different developmental times. Additionally, experiments that reverse the endogenous Notch signals would help determine whether the effects we observed represented a role of endogenous Notch signals or reflected a potential of precursors to respond to activated Notch signals.

Olfactory neurogenesis and Notch signals

Cells destined for the OB derive from the anterior region of the dorsal telencephalon following a signal initiated by primary olfactory axons (Gong and Shipley, 1995), and this neurogenesis continues into adulthood (Bayer, 1980). Our studies of postnatal injections of activated Notch1 virus into the SVZa further elucidate the difference in response to Notch signals of olfactory and cortical precursors as the precursors of the OB become more specialized. The postnatal SVZa represents a refined zone with an extremely rapid proliferation rate (Smith and Luskin, 1998) that gives rise to neurons alone, in contrast to the adjacent SVZ, which generates glia postnatally (Levison and Goldman, 1993) and retains the capacity to give rise to neurons in vitro (Reynolds and Weiss, 1992). Moreover, SVZa cells retain their commitment to

proliferate and migrate independently of radial glia, even after transplantation into the forebrain SVZ (Brock et al., 1998). We observed a virtual abolition of maturation into migrating cells destined for the OB in response to activated Notch1; this effect was more marked in the postnatal injections where no mature cells arose than in the prenatal studies, where a few neurons and glia were generated. Thus, these studies reveal a further difference between cortical and OB precursors in their response to Notch1 signals. Additionally, the precursors of the OB show a shift in their response to Notch signals as they mature from neuron- and glia-generating cells, to the neuron-only precursors in the postnatal SVZa. These conclusions must be tempered by the fact that we did not study the influence of Notch signals on cell death or proliferation of olfactory precursors after embryonic injections.

Although cortical precursors and olfactory precursors show differences in their response to Notch signals in their ultimate fates, Notch signals do appear to have a common effect on neural precursors. We note the similarity in the quiescence and lack of apoptosis elicited by Notch signals of cortical precursor cells in our short-term cultures and postnatal SVZa cells. In the latter case, however, the quiescence appears to be a permanent response to Notch signals. The cells in the postnatal SVZa that express activated Notch1 had a morphology, localization and quiescence similar to undifferentiated precursor cells or stem cells. However, these cells have not been characterized in detail. Intriguingly, in the adult SVZ, kinetic and clonal studies have indicated that very large clones are generated from quiescent stem-like cells, some of which have been shown to express GFAP (Doetsch et al., 1999; Morshead et al., 1994; Morshead et al., 1998). The similarities between adult stem cells and the response of postnatal SVZa cells to Notch suggest a model in which Notch signals serve to maintain specific precursors in an undifferentiated or stem-like state. Understanding the role of Notch signals in the control of neural stem cells may therefore be important for using stem cells in the therapy of CNS disorders and injuries.

We thank R. Axel for his early support of this project; P. Mombaerts for TLZ plasmids; Z. Z. Bao, C. Cepko and L. Lillien for viral vectors and assistance producing virus; and Fred Rademaker for assistance with the statistical analysis. Thanks to Sally Temple and Elizabeth Grove for helpful discussions, and to J. Kessler, W. Fu and N. Israsena for advice on primary neuronal cultures. We also thank the anonymous reviewers for suggestions that led to the improvement of this study. This work was supported by the March of Dimes, NIH NS35566 and a HHMI RRA award to Northwestern University. C. B. C. was supported by T32AG00260.

REFERENCES

- Artavanis-Tsakonas, S., Matsuno, K. and Fortini, M. E. (1995). Notch signaling. *Science* **268**, 225-232.
- Bao, Z. Z. and Cepko, C. L. (1997). The expression and function of Notch pathway genes in the developing rat eye. *J. Neurosci.* **17**, 1425-1434.
- Bayer, S. A. (1980). Development of the hippocampal region in the rat. I. Neurogenesis examined with 3H-thymidine autoradiography. *J. Comp. Neurol.* **190**, 87-114.
- Boulder Committee. (1970). Embryonic vertebrate central nervous system: revised terminology. The Boulder Committee. *Anat. Rec.* **166**, 257-261.
- Brock, S. C., Bonsall, J. and Luskin, M. B. (1998). The neuronal progenitor cells of the forebrain subventricular zone: intrinsic properties in vitro and following transplantation. *Methods* **16**, 268-281.

- Brunjes, P. C. and Armstrong, A. M.** (1996). Apoptosis in the rostral migratory stream of the developing rat. *Brain Res. Dev. Brain Res.* **92**, 219-222.
- Cagan, R. L. and Ready, D. F.** (1989). Notch is required for successive cell decisions in the developing *Drosophila* retina. *Genes Dev.* **3**, 1099-1112.
- Caviness, V. S.** (1982). Neocortical histogenesis in normal and reeler mice. *Dev. Brain Res.* **4**, 293-302.
- Cepko, C., Ryder, E. F., Austin, C. P., Walsh, C. and Fekete, D. M.** (1995). Lineage analysis using retrovirus vectors. *Methods Enzymol.* **254**, 387-419.
- Chitnis, A., Henrique, D., Lewis, J., Ish-Horowicz, D. and Kintner, C.** (1995). Primary neurogenesis in *Xenopus* embryos regulated by a homologue of the *Drosophila* neurogenic gene Delta. *Nature* **375**, 761-766.
- Coffman, C. R., Skoglund, P., Harris, W. A. and Kintner, C. R.** (1993). Expression of an extracellular deletion of Xotch diverts cell fate in *Xenopus* embryos. *Cell* **73**, 659-671.
- Doetsch, F., Caille, I., Lim, D. A., Garcia-Verdugo, J. M. and Alvarez-Buylla, A.** (1999). Subventricular zone astrocytes are neural stem cells in the adult mammalian brain. *Cell* **97**, 703-716.
- Dorsky, R. L., Chang, W. S., Rapaport, D. H. and Harris, W. A.** (1997). Regulation of neuronal diversity in the *Xenopus* retina by Delta signalling. *Nature* **385**, 67-70.
- Franklin, J. L., Berechid, B. E., Cutting, F. B., Presente, A., Chambers, C. B., Foltz, D. R., Ferreira, A. and Nye, J. S.** (1999). Autonomous and non-autonomous regulation of neurite development by Notch1 and Delta1. *Curr. Biol.* **9**, 1448-1457.
- Furukawa, T., Mukherjee, S., Bao, Z. Z., Morrow, E. M. and Cepko, C. L.** (2000). *rax*, *Hes1*, and *notch1* promote the formation of Muller glia by postnatal retinal progenitor cells. *Neuron* **26**, 383-394.
- Gaiano, N., Kohtz, J. D., Turnbull, D. H. and Fishell, G.** (1999). A method for rapid gain-of-function studies in the mouse embryonic nervous system. *Nat. Neurosci.* **2**, 812-819.
- Gaiano, N., Nye, J. S. and Fishell, G.** (2000). Radial glial identity is promoted by Notch1 signaling in the murine forebrain. *Neuron* **26**, 395-404.
- Ghosh, A. and Greenberg, M. E.** (1995). Distinct roles for bFGF and NT-3 in the regulation of cortical neurogenesis. *Neuron* **15**, 89-103.
- Gong, Q. and Shipley, M. T.** (1995). Evidence that pioneer olfactory axons regulate telencephalon cell cycle kinetics to induce the formation of the olfactory bulb. *Neuron* **14**, 91-101.
- Hartenstein, V. and Posakony, J. W.** (1990). A dual function of the Notch gene in *Drosophila* sensillum development. *Dev. Biol.* **142**, 13-30.
- Henrique, D., Hirsinger, E., Adam, J., Le Roux, I., Pourquie, O., Ish-Horowicz, D. and Lewis, J.** (1997). Maintenance of neuroepithelial progenitor cells by Delta-Notch signalling in the embryonic chick retina. *Curr. Biol.* **7**, 661-670.
- Jacobson, M.** (1991). *Developmental Neurobiology*. New York: Plenum Press.
- Jan, Y.-N. and Jan, L.-Y.** (1990). Genes required for specifying cell fates in *Drosophila* embryonic sensory nervous system. *Trends in Neurosci.* **13**, 493-498.
- Johe, K. K., Hazel, T. G., Muller, T., Dugich-Djordjevic, M. M. and McKay, R. D.** (1996). Single factors direct the differentiation of stem cells from the fetal and adult central nervous system. *Genes Dev.* **10**, 3129-3140.
- Levison, S. W. and Goldman, J. E.** (1993). Both oligodendrocytes and astrocytes develop from progenitors in the subventricular zone of postnatal rat forebrain. *Neuron* **10**, 201-212.
- Levison, S. W., Chuang, C., Abramson, B. J. and Goldman, J. E.** (1993). The migrational patterns and developmental fates of glial precursors in the rat subventricular zone are temporally regulated. *Development* **119**, 611-622.
- Lewis, J.** (1996). Neurogenic genes and vertebrate neurogenesis. *Curr. Opin. Neurobiol.* **6**, 3-10.
- Lillien, L.** (1995). Changes in retinal cell fate induced by overexpression of EGF receptor. *Nature* **376**, 158-162.
- Lindsell, C. E., Boulter, J., diSibio, G., Gossler, A. and Weinmaster, G.** (1996). Expression patterns of Jagged, Delta1, Notch1, Notch2, and Notch3 genes identify ligand-receptor pairs that may function in neural development. *Mol. Cell. Neurosci.* **8**, 14-27.
- Luskin, M. B.** (1993). Restricted proliferation and migration of postnatally generated neurons derived from the forebrain subventricular zone. *Neuron* **11**, 173-189.
- Marin-Padilla, M.** (1978). Dual origin of the mammalian neocortex and evolution of the cortical plate. *Anat. Embryol.* **152**, 109-126.
- McConnell, S. K.** (1988). Fates of visual cortical neurons in the ferret after isochronic and heterochronic transplantation. *J. Neurosci.* **8**, 945-974.
- Mombaerts, P., Wang, F., Dulac, C., Chao, S. K., Nemes, A., Mendelsohn, M., Edmondson, J. and Axel, R.** (1996). Visualizing an olfactory sensory map. *Cell* **87**, 675-686.
- Morrison, S. J., Perez, S. E., Qiao, Z., Verdi, J. M., Hicks, C., Weinmaster, G. and Anderson, D. J.** (2000). Transient Notch activation initiates an irreversible switch from neurogenesis to gliogenesis by neural crest stem cells. *Cell* **101**, 499-510.
- Morshead, C. M. and van der Kooy, D.** (1992). Postmitotic death is the fate of constitutively proliferating cells in the subependymal layer of the adult mouse brain. *J. Neurosci.* **12**, 249-256.
- Morshead, C. M., Reynolds, B. A., Craig, C. G., McBurney, M. W., Staines, W. A., Morassutti, D., Weiss, S. and van der Kooy, D.** (1994). Neural stem cells in the adult mammalian forebrain: a relatively quiescent subpopulation of subependymal cells. *Neuron* **13**, 1071-1082.
- Morshead, C. M., Craig, C. G. and van der Kooy, D.** (1998). In vivo clonal analyses reveal the properties of endogenous neural stem cell proliferation in the adult mammalian forebrain. *Development* **125**, 2251-2261.
- Nye, J. S. and Kopan, R.** (1995). Developmental signaling. Vertebrate ligands for Notch. *Curr. Biol.* **5**, 966-969.
- Nye, J. S., Kopan, R. and Axel, R.** (1994). An activated Notch suppresses neurogenesis and myogenesis but not gliogenesis in mammalian cells. *Development* **120**, 2421-2430.
- Paterson, J. A., Privat, A., Ling, E. A. and Leblond, C. P.** (1973). Investigation of glial cells in semithin sections. 3. Transformation of subependymal cells into glial cells, as shown by radioautography after 3 H-thymidine injection into the lateral ventricle of the brain of young rats. *J. Comp. Neurol.* **149**, 83-102.
- Qian, X., Davis, A. A., Goderie, S. K. and Temple, S.** (1997). FGF2 concentration regulates the generation of neurons and glia from multipotent cortical stem cells. *Neuron* **18**, 81-93.
- Renfranz, P. J., Cunningham, M. G. and McKay, R. D.** (1991). Region-specific differentiation of the hippocampal stem cell line HiB5 upon implantation into the developing mammalian brain. *Cell* **66**, 713-729.
- Reynolds, B. A. and Weiss, S.** (1992). Generation of neurons and astrocytes from isolated cells of the adult mammalian central nervous system. *Science* **255**, 1707-1710.
- Sestan, N., Artavanis-Tsakonas, S. and Rakic, P.** (1999). Contact-dependent inhibition of cortical neurite growth mediated by notch signaling. *Science* **286**, 741-746.
- Shellenbarger, D. L. and Mohler, J. D.** (1978). Temperature sensitive periods and autonomy of pleiotropic effects of I(1)Nts1, a conditional lethal Notch in *Drosophila*. *Dev. Biol.* **62**, 432-446.
- Shihabuddin, L. S., Hertz, J. A., Holets, V. R. and Whittemore, S. R.** (1995). The adult CNS retains the potential to direct region-specific differentiation of a transplanted neuronal precursor cell line. *J. Neurosci.* **15**, 6666-6678.
- Simpson, P. and Carteret, C.** (1990). Proneural clusters: equivalence groups in the epithelium of *Drosophila*. *Development* **110**, 927-932.
- Smith, C. M. and Luskin, M. B.** (1998). Cell cycle length of olfactory bulb neuronal progenitors in the rostral migratory stream. *Dev. Dyn.* **213**, 220-227.
- Snyder, E. Y., Deitcher, D. L., Walsh, C., Arnold-Aldea, S., Hartweg, E. A. and Cepko, C. L.** (1992). Multipotent neural cell lines can engraft and participate in development of mouse cerebellum. *Cell* **68**, 33-51.
- Suhonen, J. O., Peterson, D. A., Ray, J. and Gage, F. H.** (1996). Differentiation of adult hippocampus-derived progenitors into olfactory neurons in vivo. *Nature* **383**, 624-627.
- Wakamatsu, Y., Maynard, T. M., Jones, S. U. and Weston, J. A.** (1999). Numb localizes in the basal cortex of mitotic avian neuroepithelial cells and modulates neuronal differentiation by binding to NOTCH-1. *Neuron* **23**, 71-81.
- Zhong, W. M., Jiang, M. M., Weinmaster, G., Jan, L. Y. and Jan, Y. N.** (1997). Differential expression of mammalian Numb, numb-like and Notch1 suggests distinct roles during mouse cortical neurogenesis. *Development* **124**, 1887-1897.
- Zhu, G., Mehler, M. F., Zhao, J., Yu Yung, S. and Kessler, J. A.** (1999). Sonic hedgehog and BMP2 exert opposing actions on proliferation and differentiation of embryonic neural progenitor cells. *Dev. Biol.* **215**, 118-129.